Rayapati Subbarao* and M. Govardhan

Studies on the Effect of Staggering the Rear Rotor in a Counter Rotating Turbine with Respect to Flow and Performance Parameters

DOI 10.1515/tjj-2016-0061
Received September 15, 2016; accepted October 30, 2016

Abstract: Counter rotating turbine is an axial turbine with nozzle followed by a rotor and another rotor that rotates in the opposite direction of the first one. Absence of the second guide vane makes it more beneficial. Present work involves computationally studying the performance and flow pattern of CRT with different stagger angles ranging from 8 to 13° in case of rotor 2. Equivalent mass flow rates of 0.091 to 0.137 are considered. Turbine components nozzle, rotor 1 and rotor 2 are modeled for the cases of CRT with and without staggering. Total pressure, entropy and TKE distributions across the blade rows are used to describe the flow through CRT. Results show that the flow composition at the inlet of rotor 2 is improved for staggering cases. Due to this, the performance of rotor 2 and CRT increased with staggering. For the intermediate mass flow rate of 0.108, the efficiency of CRT stage is found to be increasing by 1.2, 2.1 and 1% for the staggering cases. The beneficial aspect of staggering the rear rotor is thus confirmed that can provide long-term design solutions in terms of reducing weight, losses and improving the performance.

Keywords: counter rotating turbine (CRT), stagger angle, turbine performance, losses, mass flow rate

PACS® (2010). 47.85.Gj, 47.11.-j, 47.27.E-

Introduction

Conventional axial turbine consists of stationary vanes (nozzles) and rotating blade rows (rotors) consequently placed. Increasing demand for the improvement of efficiency, reduction of weight and consideration of fuel consumption in case of power generation lead the researchers to arrive at an unconventional turbine known as Counter Rotating Turbine (CRT) that has two rotors. In case of CRT, nozzle is followed by a rotor and another rotor that rotates in the opposite direction of the first one. Because of the unconventional architecture and absence of the second guide vane, it offers advantages on weight, volume and efficiency. It can perform even better in wide range of rotation speeds. Mere 1% improvement in the efficiency would save millions of dollars. Such placement of flow elements gives benefits, but attention must be paid to the selection of optimal rotation speed and flow conditions. CRT with two rotors that have different rotational speeds and power to drive accessories is being applied for rocket engines. This configuration avoids the disadvantages of gearbox and two turbine pattern. CRT finds applications in aeronautic, astronautic fields and in military applications. Now, several countries are developing CRTs for aircrafts and in some advanced active duty aero-engines. Earlier, efficiency of a two-stage CRT was analyzed in terms of work and speed requirements by Wintucky and Stewart [1]. It was assumed that the advantage aspect might be due to the removal of inter-stage stator. Ozgur and Nathan [2] considered a particular counter rotating turbine stage with and without guide vanes that has axial inlet and outlet velocities, equal rotation speeds and specific work in each blade row. Louis [3] analyzed both the types of CRTs and found that stage loading coefficients were higher when compared with the conventional one. To improve the performance of CRT, there have been many parameters that can be studied. Ji et al. [4] were the first to investigate the work capability of CRT computationally and found specific work ratio and flow angle as important parameters. There have been many such parameters that affect the performance of a turbine.

Duncan and Dawson [5] adopted staggering of rotor blades in an axial flow fan in order to obtain reduction of tonal annoyance when the reduction expected from a judicious choice of blade and vane numbers could not be fully realized. Sharma et al. [6] studied the effect of second rotor staggering in a contra-rotating axial compressor stage. The stagger setting of the second rotor

***Corresponding author: Rayapati Subbarao,** Department of Mechanical Engineering, Indian Institute of Technology Madras, Chennai 600036, Tamil Nadu, India,
E-mail: rsubbarao@hotmail.com
M. Govardhan, Department of Mechanical Engineering, Indian Institute of Technology Madras, Chennai 600036, Tamil Nadu, India

and also its speed strongly influenced the performance of both first rotor and the stage. Shigemitsu et al. [7] found new design to decrease rear rotor's stagger angle that resulted in the stable operation of a pump. Tang et al. [8] obtained the influence of work ratio of both the rotors on high pressure stage efficiency in case of turbo pump. In case of aircraft engines, high work-ratio meets the requirement of rocket turbo pump, where increased work ratio leads to increased efficiency. Effect of stagger angle in an axial compressor stage was studied by Ramakrishna and Govardhan [9]. Flow separation and shifting of stall point were observed with change in stagger angle. Different cases discussed on staggering here are concerned with design details on how to stagger blades to reduce noise, shifting stall point and stabilize the operation. Effect of staggering is not studied earlier by researchers in case of counter rotating turbines, where the significance of changing the stagger angle is very different from other mentioned instances. The purpose of staggering in the present work is to ensure reduced flow losses at the rotor 1 – rotor 2 interface that may positively affect the performance of rotor 2 and the overall CRT stage. The effect of staggering the rear rotor by 8–13° is studied here, aiming flow and performance analysis. CRT represents the case without the staggering of rotor 2. Staggered CRT cases are referred as CRTS8, CRTS10 and CRTS13.

Methodology

Geometry preparation and meshing

CRT stage considered in the present work consists of 22, 28 and 28 blades of nozzle, rotor 1 and rotor 2 respectively. Modeling and meshing of the computational domain are done using the commercial software ANSYS® ICEM CFD 14.0. Computational domain of CRT contains nozzle, rotor 1 and rotor 2 as shown in Figure 1(a). Modified details of the geometric configuration obtained from Dring et al. [10] are shown in Table 1. Axial gap between the blade rows of nozzle –2 rotor 1 and rotor 1 – rotor 2 is taken as 30 % of the average of the nozzle and rotor axial chords, on the basis of the earlier work done by the same authors [11]. At this gap, CRT configuration under study is showing higher performance. Tip clearance of 2.28 mm, which is about 1.5 % span, is provided on both the rotors. Table 2 shows the details of nozzle and rotor profiles at the midspan section. Same profile is used for both the rotors. X-axis is chosen as the axis of revolution. Flow is treated as periodic and domain of the nozzle is taken with three blades and that of rotors is taken with four blades to maintain pitch ratio close to 1 in order to minimize approximations of the numerical simulation. The positions of rotor 2 before and after staggering are shown in Figure 1(b). The selected range of staggering is based on the incidence angle of the flow at second rotor for the intermediate mass flow rate, considering performance in case of CRT. Figure 2(a) shows the variation of turbine stage efficiency with mass flow rate without staggering. For the flow rate of 0.108, the efficiency of CRT is maximum. Incidence angle variation for the same configuration with different flow rates is as shown in Figure 2(b). The selected region of mass flow rate is showing the negative incidence in the range of 8 to 13°. Accordingly, the second rotor is staggered in the present study. The angle between the chord line and the turbine axial direction is varied by stagger angle, changing the blade position with respect to vertical axis.

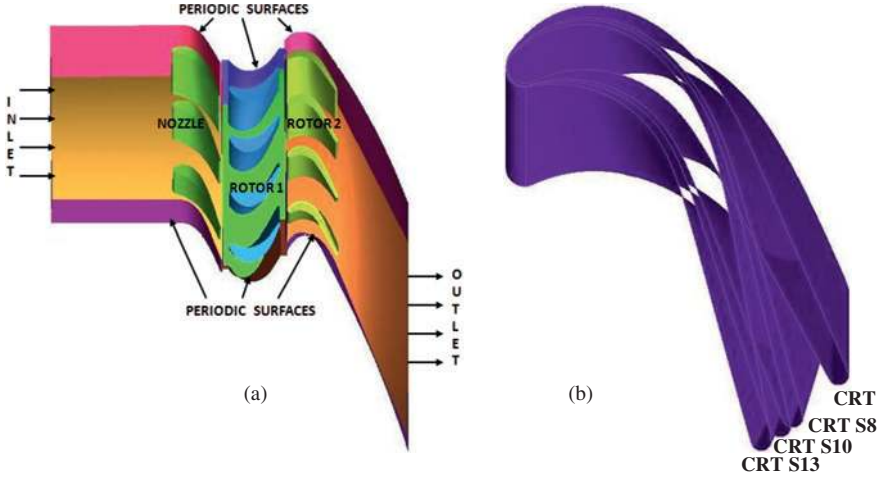

Figure 1: Computational domain of CRT and staggering of rotor 2.

Table 1: Blade configuration used in CRT.

Parameter	Nozzle	Rotor 1	Rotor 2
Number of blades	22	28	28
Hub radius (mm)	610	610	610
Tip radius (mm)	762–776	776–790	790–805
Tip clearance (mm)	0	2.28	2.28

Table 2: Details of nozzle and rotor profiles at the midspan section.

Details	Nozzle	Rotor
Axial chord (mm)	151	161
Blade spacing (mm)	195.11	154.9
Space-chord (s/ch) ratio	0.85	0.85
Blade inlet angle	90°	138°
Blade exit angle	21.42°	25.97°
Stagger angle	49.56°	31.59°
Deflection angle	68.58°	111.85°

For grid generation, tetra meshing is used. For improved mesh quality, it incorporates a powerful smoothening algorithm as well as tools for local adaptive mesh refinement and coarsening. For better modeling of near-wall physics of the flow pattern, prism meshing is done that consists of layers near the boundary surfaces and tetrahedral elements in the interior. Mesh distribution is done to provide sufficiently large number of elements near the blade, leading and trailing edges as shown in Figure 3(a) for the case of nozzle. The presence of prism layers around the blades and the growth of prism layers, according to the height ratio can be seen in the figures. The interior part will have relatively less dense mesh compared to the mesh near the blade, hub and shroud. Capturing of the edges and the growth of the mesh from walls to the blade and the interior zone has been excellent as seen in the nozzle mesh. Same method is followed for rotor 1 and rotor 2 as well. Close view of the mesh for all the three blades and the CRT domain is shown in Figure 3(b). Number of mesh elements for nozzle, rotor 1 and rotor 2 are given in Table 3. The number of elements for nozzle and rotor 1 will remain same in all the configurations. Elements in rotor 2 vary with stagger angle as shown. Nodes will vary according to the mesh size. For example, in case of rotor 2, there are 2.02 million nodes for about 5.52 million mesh size in CRT case. Once mesh of set quality is obtained, all the three components are imported to CFX 14.0, which is used for solving and post processing.

Boundary conditions

Total pressure at nozzle inlet and mass flow rate at rotor 2 outlet are specified as boundary conditions. Details of flow parameters are shown in Table 4. Equivalent mass flow rates are obtained by normalizing the mass flow rate based on the inlet conditions. Inlet flow is assumed to be uniform with no swirl. Air as ideal gas is considered as the working fluid. All surfaces viz. hub, tip and the blade are given smooth wall with no-slip boundary condition. Rotational periodicity is enforced about the axis of rotation. Frozen rotor interface is used for rotor-stator frame change interface. Rotational speed of the rotors is 600 RPM. Rotor 1 rotates in the clockwise direction when observed from the upstream of the rotor. Rotor 2 rotates with the same speed, but in the anti-

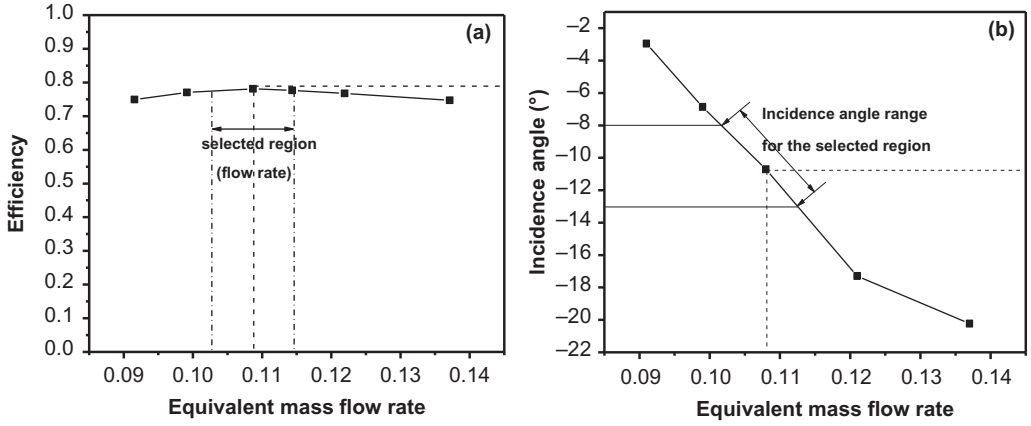

Figure 2: Efficiency of CRT and incidence angle at rotor 2 inlet, without staggering.

(a) (b)

Figure 3: Close view of the mesh near LE, TE, nozzle and the CRT.

Table 3: Details of mesh elements.

Details	Number of elements			
	CRT	CRTS8	CRTS10	CRTS13
Nozzle	3,745,306	3,745,306	3,745,306	3,745,306
Rotor 1	3,820,062	3,820,062	3,820,062	3,820,062
Rotor 2	5,524,652	4,990,415	4,892,484	4,625,046

Table 4: Flow parameters used in the simulation.

Parameter	Value
Inlet temperature (K)	480
Total pressure at the inlet (Pa)	1.35×10^5
Equivalent mass flow rate	0.091–0.137
Working fluid	Air ideal gas
Inlet turbulence (%)	1
Speed of rotors	600

clockwise direction, opposite to the first rotor. Based on the inlet boundary condition, turbulence intensity of the incoming flow is considered as 1% for all the configurations. Reference pressure is taken as 1 ata. Convergence criteria of target RMS residual value is set as 10^{-4}. Standard k–ω based Shear Stress Transport (SST) turbulence model is used.

Results and discussion

Flow through the turbine stage is complex and the objective of the present work is to present and analyze the features of flow pattern with staggering at the exit of rotor 1 and rotor 2 that affect the performance of the CRT stage. Total pressure, entropy and Turbulent Kinetic Energy (TKE) are taken as variables to describe the flow. These parameters are plotted at the inlet and outlet axial planes of the blade rows. Planes before and after the blade rows are taken at a distance of half of the intermediate axial gap. Pressures are normalized by the total pressure at turbine inlet. Entropy is normalized by gas constant. Static Enthalpy Loss Coefficient (SELC) gives the measure of enthalpy losses, normalized by dynamic head. TKE is normalized by the square of velocity. SELC and TKE are used as parameters that represent losses. Efficiency is defined as the ratio of the power output obtained from the rotor torque to the input based on total enthalpy drop across the stage. Torque obtained from rotors and the efficiency are taken as performance indices to compare different configurations of CRT.

Grid independent study and validation

Grid independence study is carried out in order to ensure that the results are not dependent on changes in the grid size. This study is performed by altering the number of mesh elements with the help of global mesh parameter variation. For different grid sizes, Figure 4 shows the pressure coefficient of rotor, which is determined from the difference of the blade surface and reference pressure at the inlet of the blade normalized by the inlet dynamic pressure. As the mesh size is increased from 3.0 to 3.6 millions, pressure coefficient is observed as increasing. When the mesh size is raised further, no change in pressure coefficient is observed. Thus, for rotor, the mesh of 3.6 million elements is chosen, as there is no variation of the measured variable further

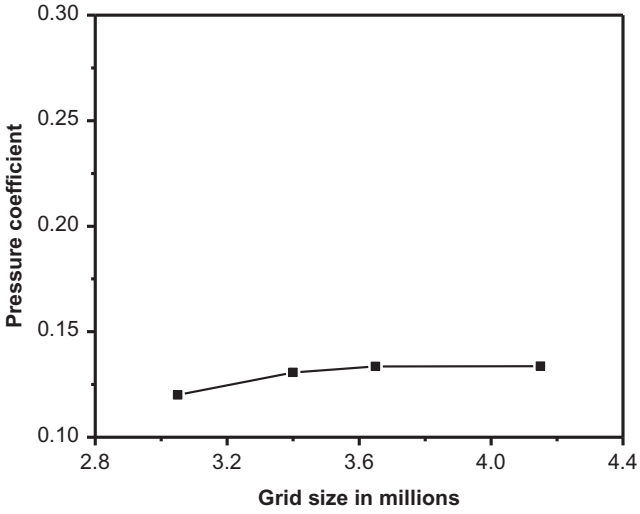

Figure 4: Grid independence study of rotor.

with change in mesh size. This also ensures that computational time is saved and flow physics is accurately captured. Thus, grid independence study takes care of the optimized mesh size, computational time and variation of selected flow or performance variable. Simulation results are compared with the experimental results of Dring et al. [10] obtained on a large scale rotating turbine rig. Pressure coefficient distribution of rotor is used for comparison as shown in Figure 5. Pressure coefficients from computation are in good agreement except for a small region on the suction side near the trailing edge. The slight deviation near the leading is due to over prediction of simulation results. Near the trailing edge,

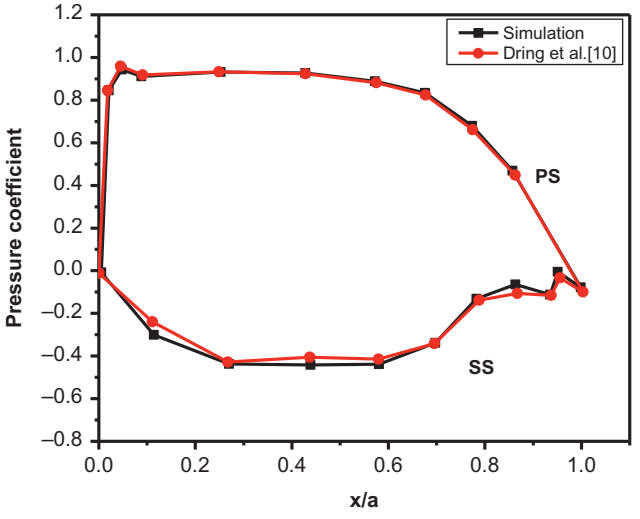

Figure 5: Pressure coefficient of rotor.

it may be due to the variation in capturing the minute edges by computational model.

Flow pattern at the exit of rotor 1 with and without staggering

In this section, variation of flow parameters is discussed at the exit of rotor 1. Normalized tangential distance (y/s) is taken on x-axis, where y is the distance in that direction and s is blade spacing. Radial distance taken on y-axis is normalized by tip radius and is represented by r/r_t. Flow near the tip region varied with staggering cases at the outlet of rotor 1 as shown in the total pressure contour of Figure 6. This is noticeable in the form of changed size and strength of the low pressure region in the wake. Position of the wake is changing with staggering. Variation of total pressure on the pressure side is comparable in CRTS10 and CRT with slight variation in magnitudes. In CRTS13, more pressure losses are observed near the wake region at the exit of rotor 1, that are expanding from hub to tip, which is not observed in CRTS8 and CRTS10. Tip side pressures are varying with staggering on the suction side region. Wake position is varying with change in the stagger angle and hence the position of low pressure region varies at the exit of rotor 1 that tends to move towards the suction side of rotor 1 as the staggering angle is increased.

Entropy at the outlet of rotor 1 shows the variation of losses with staggering as shown in Figure 7. Losses are more spread in the passage and the tip clearance in CRTS13 when compared to other cases. In CRTS10, entropy values are less compared to all other cases on the pressure and trailing edge sides of rotor 1. Contours also show that the effect of staggering on losses is less at the exit of rotor 1. On the suction side, only slight variation is observed that changed with staggering. TKE is more in CRTS13 case at the exit of rotor 1 as shown in Figure 8. In CRTS10, flow is less turbulent when compared to other cases of staggering. In all the cases, less TKE is observed on the suction side when compared to the pressure side, because of the presence of velocity variation. Flow becomes more turbulent near the tip and in the passage with increased staggering, because of which losses will be more in case of CRTS13. It is clear that the magnitude of TKE and related losses are less in CRTS10, when compared with other staggering cases. For more clarity, mass average values of TKE are also drawn at the exit of blade rows and are explained in Section 3.4.

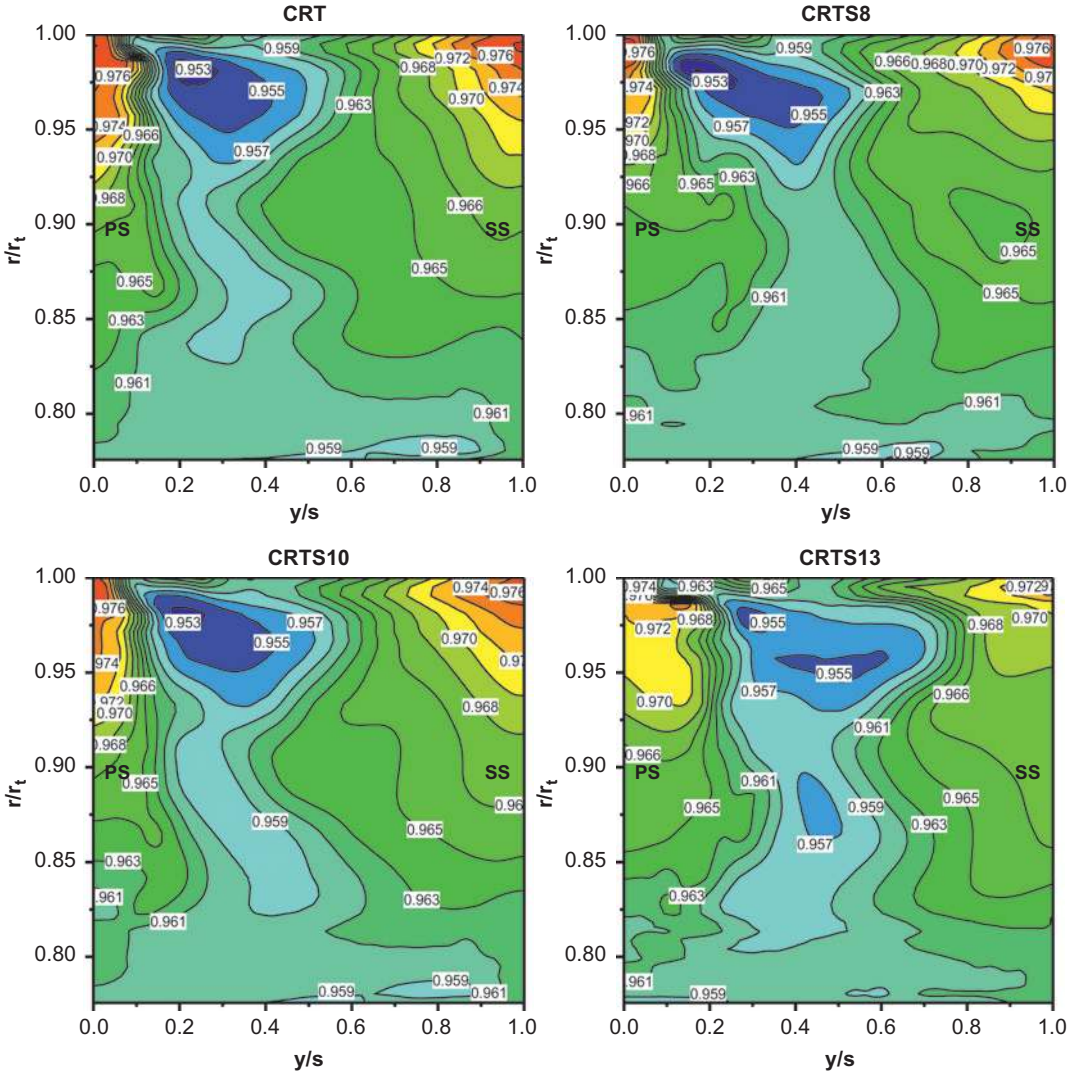

Figure 6: Total pressure variation at the outlet of rotor 1.

Flow pattern at the inlet of rotor 2 with and without staggering

Stagger angle effect on the flow in CRT stage is observed at the outlet of rotor 1 itself, as observed in the contours of flow parameters in the previous section. Since the region between the rotors is significant because of the oppositely rotating rotors, it is required to study how the flow enters rotor 2 as well. This section describes the contours drawn at the plane, just before the inlet of rotor 2. Total pressure contours shown in Figure 9 at rotor 2 inlet find pressures varying on both the sides of the blade that affect the performance of rotor 2. With staggering, useful effect is obtained in the form of less amount of fluid getting entrapped in the low pressure regions in case of CRTS10. In CRTS13, total pressures are varying much over the entire span, with peak values being less compared to other cases. This suggests the presence of more divergence in the flow at the inlet of rotor 2 with high staggering case that may affect the performance adversely. Variation on the pressure side is observed with staggering. Also, high pressures near the tip on the suction side reduce with staggering. Entropy contours at the inlet of rotor 2 are shown in Figure 10. Loss zones are similar in all the cases that extend from tip to hub, except in case of CRTS13, where high entropy regions are spread near the tip on the suction side. CRTS8 finds high entropy values near the

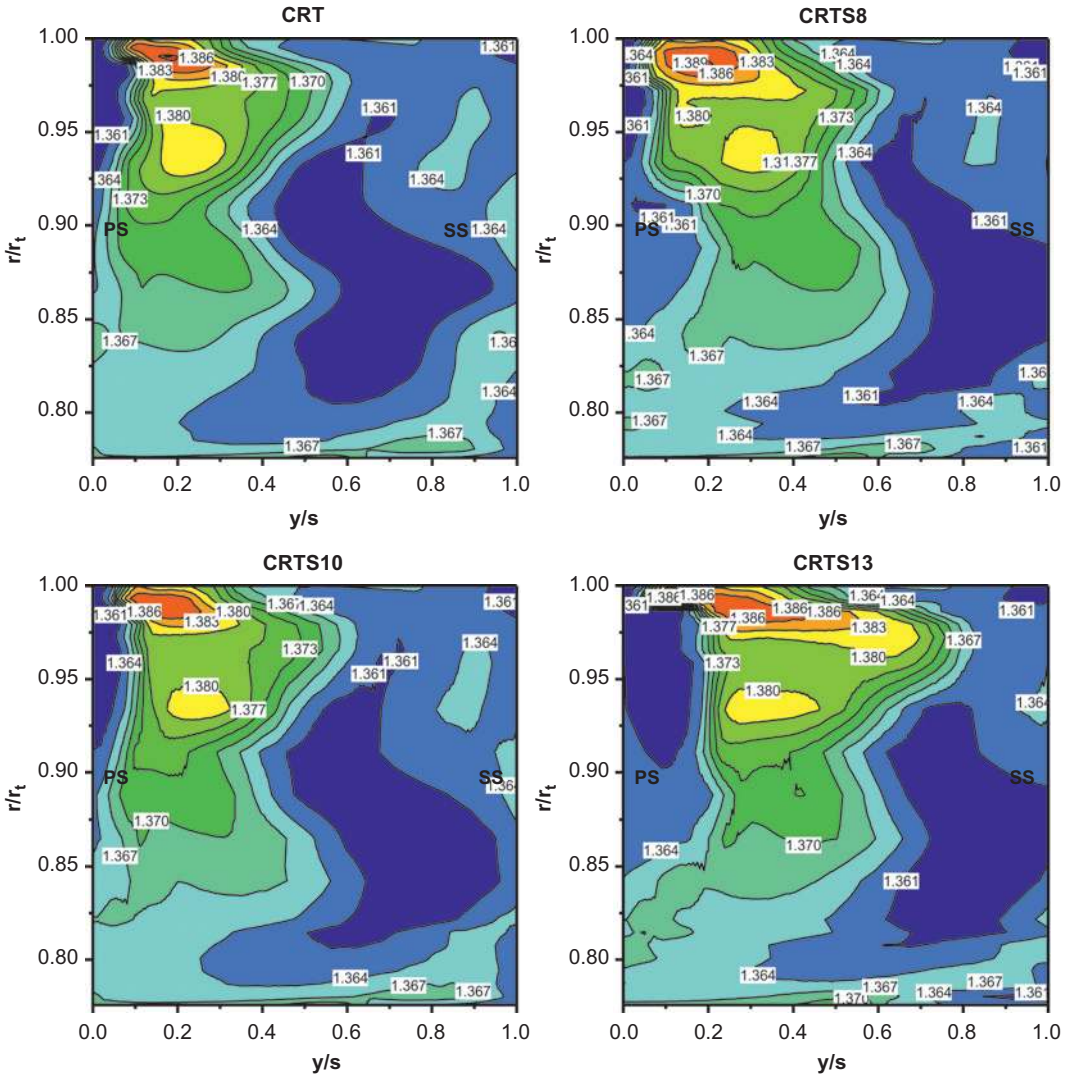

Figure 7: Entropy variation at the outlet of rotor 1.

tip compared to CRTS10. With increased stagger, losses shift towards the leading edge of rotor 2 as observed in CRTS10 case. It is observed that losses are less in CRTS10 and CRTS8. As shown in Figure 11, turbulent losses are high in CRTS13, when compared to other cases of staggering. As the flow from rotor 1 moves towards the suction side and impinges on the staggered rotor 2 blade, TKE is observed to be more on the suction side. Near the tip, this tendency is more. In case of CRTS8 and CRTS10, TKE is less and negligible when compared to the high TKE values that are observed in CRTS13 case. Peak TKE and entropy values are less in case of CRTS10, confirming the beneficial effect of staggering by 10°, where the fluid enters the second rotor with less turbulence and overall losses, obtaining more performance.

Loss parameters with and without staggering

Effect of staggering is observed in the qualitative plots of flow parameters as discussed in the earlier sections. This section is used to describe the mass averaged loss parameters at the exits of the blade rows. Static enthalpy loss coefficients at the exit of rotor 1 and rotor 2 are shown in Figure 12. In both the rotors, the effect of staggering is clear. Enthalpy losses are less in

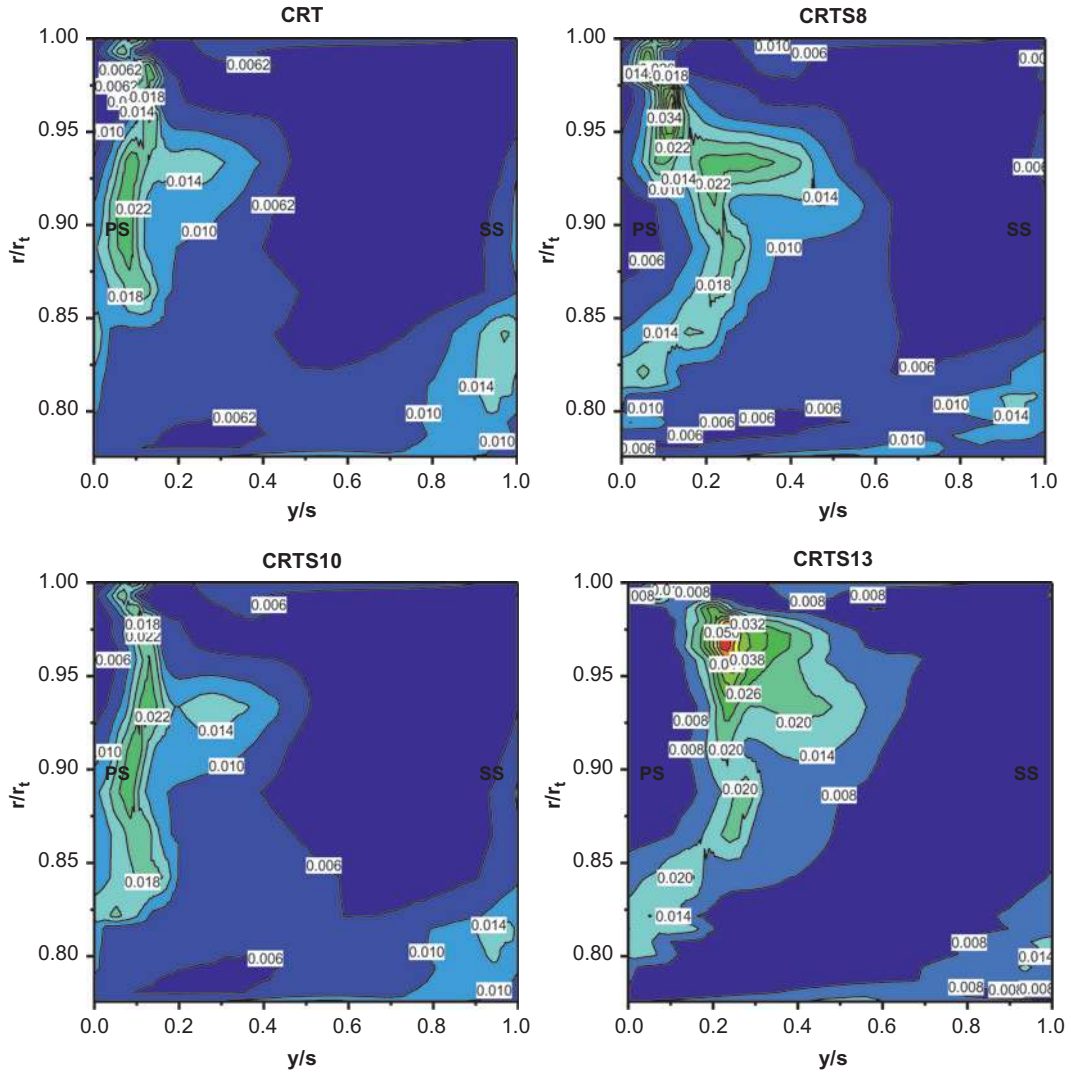

Figure 8: TKE variation at the outlet of rotor 1.

all the staggering cases than the CRT without staggering. In rotor 1, enthalpy losses increase as staggering is reduced. In case of rotor 2, these losses decrease more than rotor 1, which is the favorable effect of staggering. At the exit of rotor 2, enthalpy losses reduced with increased mass flow rate, whereas in rotor 1 enthalpy losses increase with flow rate. In CRTS13, enthalpy losses are less at the exit of both the rotors. This is observed for all the flow rates. Figure 13 shows the variation of TKE at the exit of rotor 1 and rotor 2 with staggering. TKE is more in CRTS13 at the exit of both the rotors. In rotor 2, CRTS13 shows steep rise in TKE for all the flow rates. At the exit of rotor 1, TKE values in case of CRTS8 and CRTS10 are comparable to CRT. In rotor 2, TKE is less in CRTS10 for the flow rates of 0.091 and 0.099. In CRTS8, TKE is less for the flow rates of 0.121 and 0.137. For the flow rate of 0.108, both the cases of CRTS8 and CRTS10 have same TKE at the exit of rotor 2. At the exit of rotor 2, CRTS13 shows considerably high values of TKE than the case of rotor 1.

Performance analysis with and without staggering

Torque obtained from rotor 1 and rotor 2 with staggering is plotted in Figure 14. Torque obtained from rotor 1 does not vary with the staggering of rear rotor except slightly for lesser flow rates in case of CRTS13. Torque obtained from rotor 2 increased with staggering. Increased flow

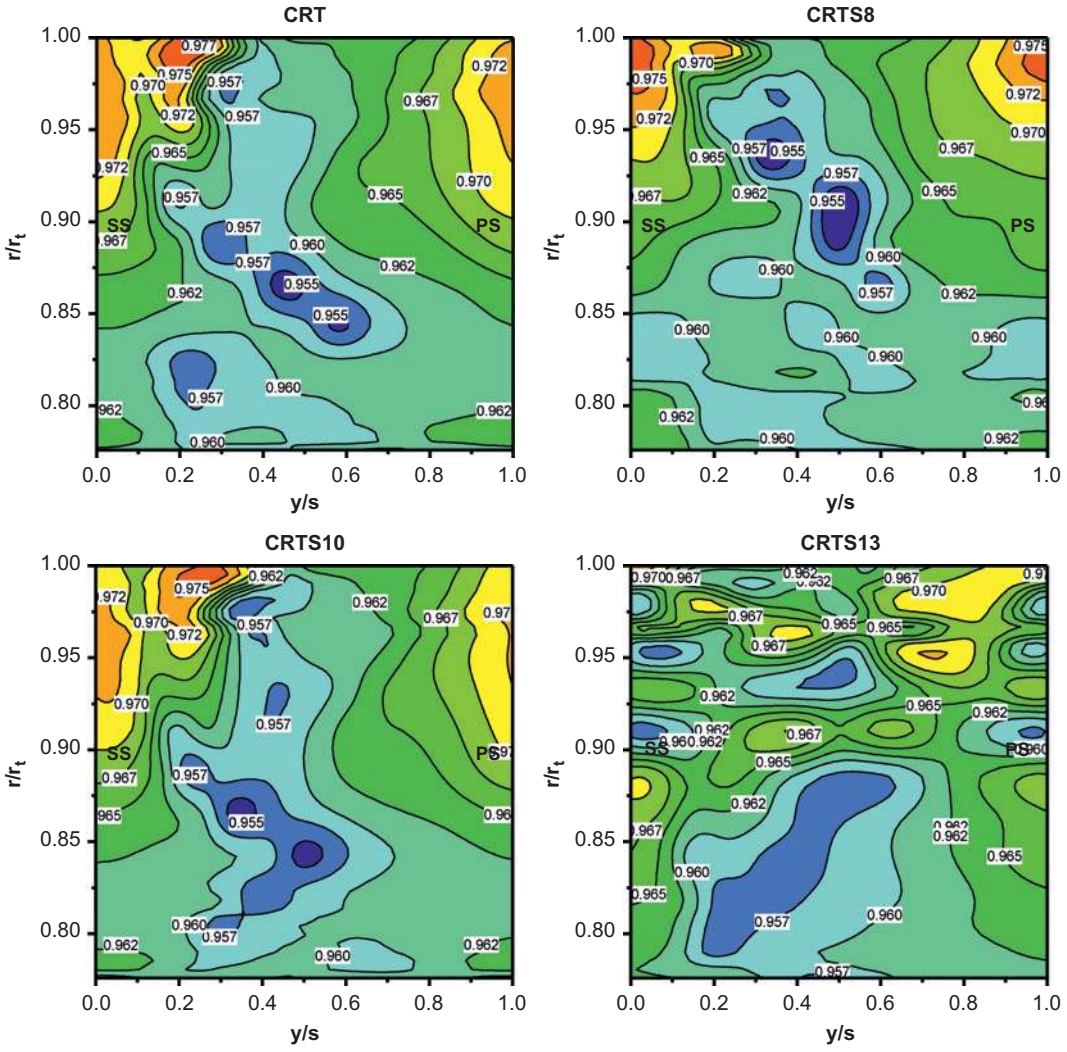

Figure 9: Total pressure variation at the inlet of rotor 2.

rate results in increased torque in both the rotors. Efficiency plots of rotor 1 and rotor 2 with flow rate are shown in Figure 15. In case of rotor 1, efficiency remained same, which shows that the effect is clearly on rotor 2 because of the staggering of the blade. Efficiency of rotor 2 is greatly increased as the stagger angle is changed from 8 to 13°. Same is with the case of CRT, the efficiency of rotor 2 is not varying much as the flow rate is increased to 0.121 and more. In case of CRTS10 and CRTS13, efficiency of rotor 2 remained same for most of the flow rates. In CRTS8, high performance is obtained from rotor 2 for the highest flow rate. The cumulative effect of all these losses and torque obtained from both the rotors is visualized in Figure 16(a) in the efficiency plot. Overall performance of the turbine is increasing in all the cases of staggering. CRTS10 shows better performance for most of flow rates than CRTS13, CRTS8 and CRT. For higher flow rates, the performance of the turbine slightly improved in CRTS8 when compared to CRTS10. In case of 0.108, at which CRT gave maximum performance before staggering is compared with other cases as shown in Figure 16(b). It is clear that staggered CRT cases showed higher performance. CRTS10 showed 2.1% higher efficiency than CRT, whereas the case of CRTS8 improved by 1.2% and CRTS13 established 1% increment. This supports the idea of staggering to capture the benefit in terms of more work obtained from the rear rotor and at the same time it could be ensured that losses are less to further enhance the performance of the turbine stage. Thus, the present work paves the way for increased number of applications while providing long term solutions of CRTs.

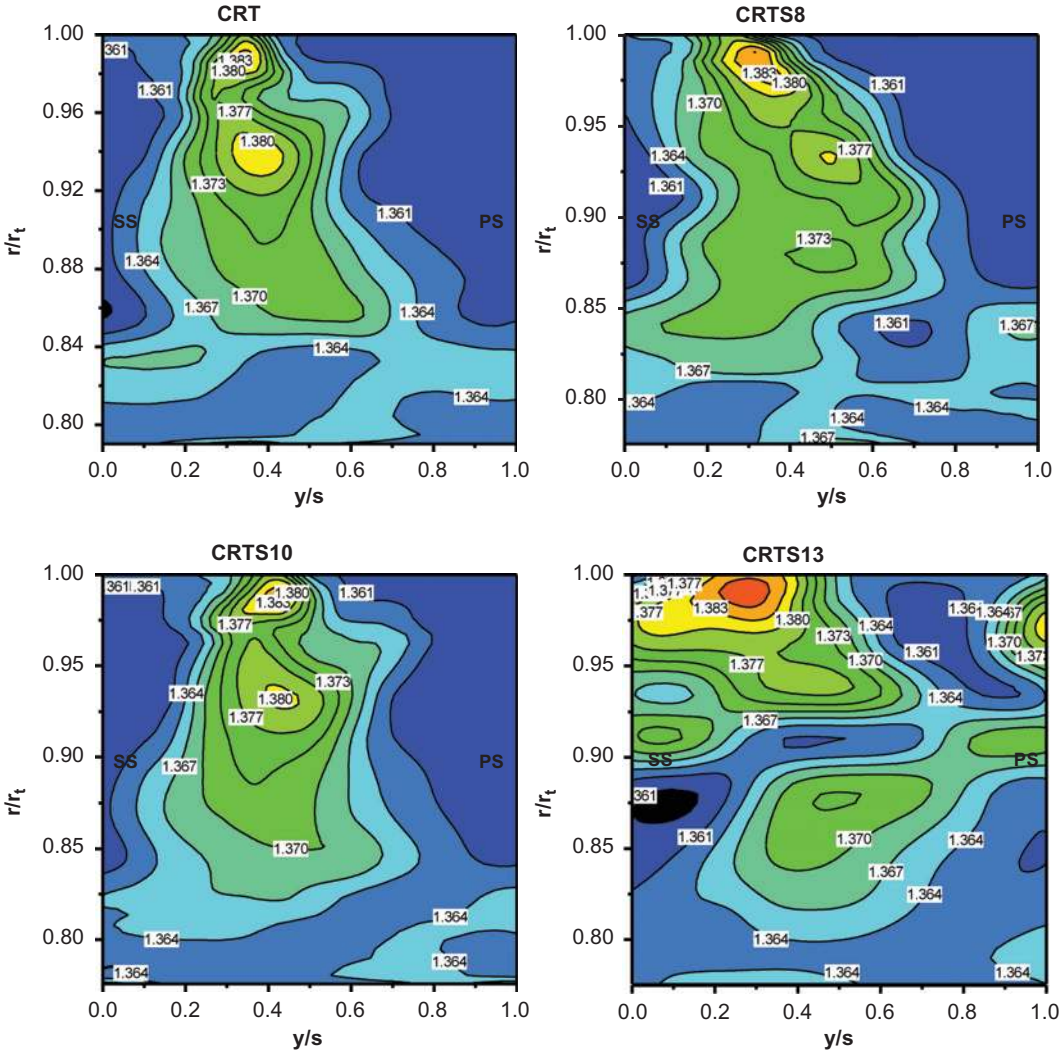

Figure 10: Entropy variation at the inlet of rotor 2.

Conclusions

Computational study is carried out on counter rotating turbine aiming aerodynamic, flow and performance aspects with the staggering of rear rotor in the range of 8–13°. Total pressure, entropy and TKE contours drawn at the exit and entry of blade rows are used to study the flow phenomena in CRT stage. Pressure, entropy and TKE contours confirm that more work is done by the first rotor than the second rotor in a counter rotating turbine. With staggering, useful effect is obtained in the form of less amount of fluid getting entrapped in the low pressure regions in CRTS8 and CRTS10. In CRTS13, pressures are varying much over the entire span, with peak values being less compared to other cases. This suggests the presence of more deviation in the flow at the inlet of rotor 2 with high staggering case that adversely affects the performance. Flow is more uniformly distributed at the leading edge of the blade with staggering that reduces losses. Overall performance of the turbine is increased in all the cases of staggering when compared to CRT without staggering. CRTS10 showed better performance for most of flow rates than all other cases of staggering as incidence, enthalpy and turbulence losses are less when compared to CRTS8 and CRTS13. For higher flow rates, the performance of the turbine slightly improved in CRTS8 when compared to CRTS10. Thus the present work supports the aspect of changing the stagger angle in order to obtain improved flow pattern at the inlet of rotor 2 and the increased performance of rotor 2 as well as that of CRT stage.

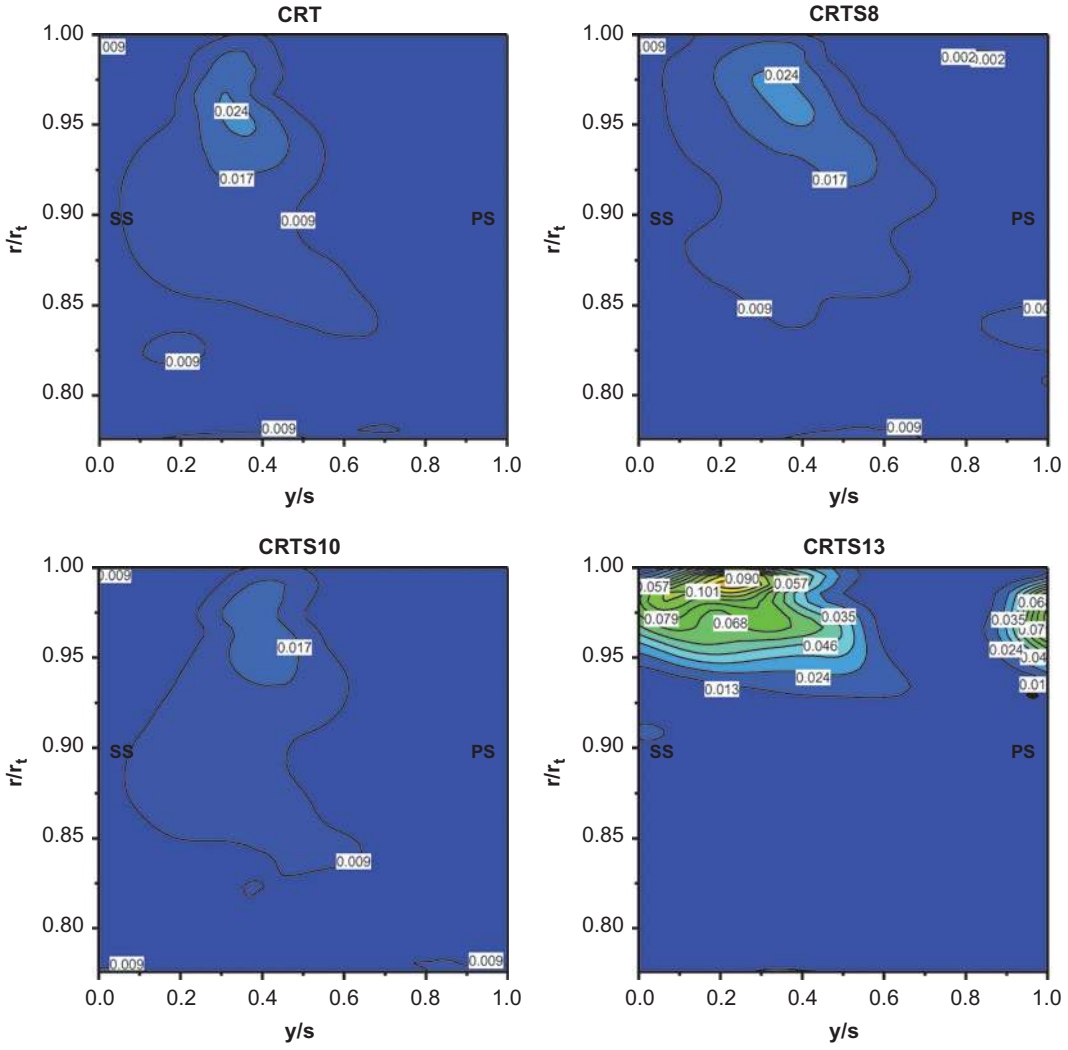

Figure 11: TKE variation at the inlet of rotor 2.

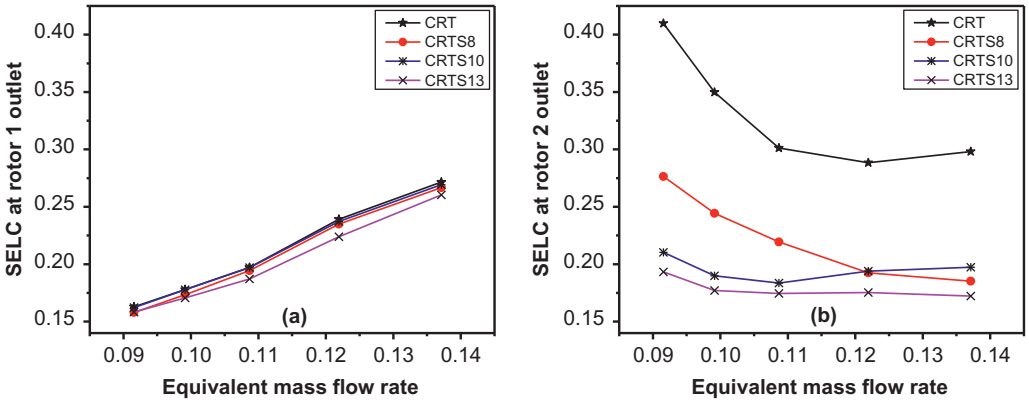

Figure 12: SELC at the outlet of rotor 1 and rotor 2.

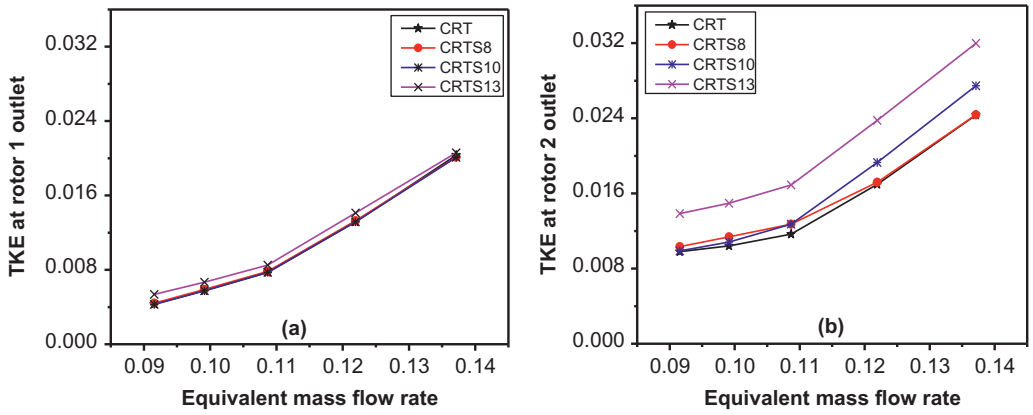

Figure 13: TKE at the outlet of rotor 1 and rotor 2.

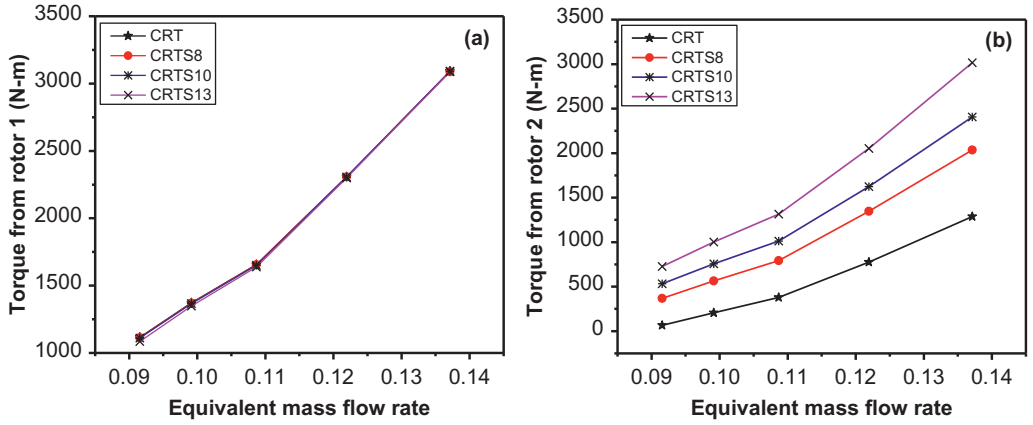

Figure 14: Torque obtained from rotor 1 and rotor 2.

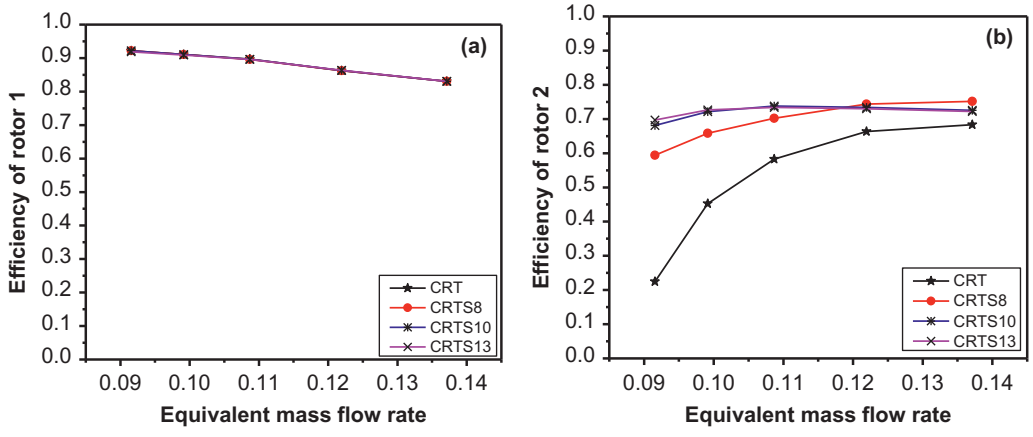

Figure 15: Efficiency of rotor 1 and rotor 2.

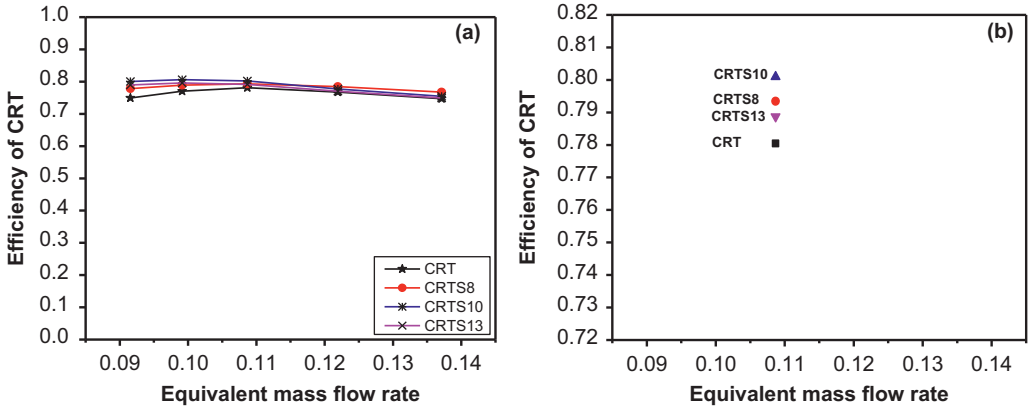

Figure 16: Efficiency of CRT with and without staggering.

Nomenclature

a	Axial chord (m)
C	Absolute velocity (m/s)
s	Blade spacing (m)
SELC	Static enthalpy loss coefficient
TKE	Turbulent kinetic energy
U	Blade speed (m/s)
W	Relative velocity (m/s)
x, y	Distance along x and y – axes (m)

References

1. Wintucky WT, Stewart WL. Analysis of two-stage counter-rotating turbine efficiencies in terms of work and speed requirements. Report NACA RM E57L05, 1957.
2. Ozgur C, Nathan GK. Study of contra-rotating turbines based on design efficiency. J Basic Eng 1971;93:395–404.
3. Louis JF. Axial flow contra-rotating turbines. ASME paper, 85-GT-218, 1985.
4. Ji LC, Quan XB, Wel L, Xu JZ. A vaneless counter rotating turbine design towards limit of specific work ratio. ISABE paper, 2001–1062, 2001.
5. Duncan PE, Dawson B. Reduction of interaction tones from axial flow fans by suitable design of rotor configuration. J Sound Vib 1974;33:143–54.
6. Sharma PB, Jain YP, Pundhir DS. A study of some factors affecting the performance of a contra-rotating axial compressor stage. Proc Inst Mech Eng A J Power Energy 1988;202:15–21.
7. Shigemitsu T, Furukawa A, Watanabe S, Okuma K, Fukutomi J. Experimental analysis of internal flow of contra-rotating axial flow pump. 8th International Symposium on Experimental and Computational Aerothermodynamics of Internal Flows, Toru, ISAIF 8–0034, 2007.
8. Ramakrishna PV, Govardhan M. Pressure rise and diffusion qualities of forward swept axial compressor rotor passages at different stagger angles. 13th Asian Congress of Fluid Mechanics, Dhaka, Bangladesh, 2010:671–4.
9. Tang F, Zhao XL, Xu JZ. The application of counter-rotating turbine in rocket turbopump. Int J Rotating Mach 2008:Article ID 426023. DOI: 10.1155/2008/426023.
10. Dring RP, Joslyn HD, Blair MF. The effect of inlet turbulence and rotor/stator interactions on the aerodynamics and heat transfer of large scale rotating turbine model. Report NASA CR 179469, 1987.
11. Subbarao R, Govardhan M. Effect of axial spacing between the components on the performance of a counter rotating turbine. Int J Fluid Mach Syst 2013;6(4):170–6.